Geoderma 160 (2011) 579–589

Contents lists available at ScienceDirect

Geoderma

journal homepage: www.elsevier.com/locate/geoderma

Atypical early-time infiltration into a structured soil near field capacity: The dynamic interplay between sorptivity, hydrophobicity, and air encapsulation

S. Carrick [a,*], G. Buchan [b], P. Almond [c], N. Smith [c]

[a] Landcare Research, PO Box 40, Lincoln 7640, New Zealand
[b] Centre for Soil and Environmental Research, Lincoln University, PO Box 84, Lincoln 7640, New Zealand
[c] Department of Soil and Physical Sciences, PO Box 84, Lincoln University, New Zealand

ARTICLE INFO

Article history:
Received 19 April 2010
Received in revised form 4 November 2010
Accepted 10 November 2010
Available online 16 December 2010

Keywords:
Sorptivity
Hydrophobicity
Air encapsulation
Early-time infiltration
Lysimeter
Tension infiltrometer

ABSTRACT

Accurate measurement of infiltration attributes for the soil's surface layer is critical for understanding the dynamics of soil water in response to rainfall or irrigation. This study used four large lysimeters to measure the early-time infiltration behaviour of a structured, well-drained, silt loam Dystric Cambisol. For each lysimeter there were four separate infiltration experiments, with a 480-mm-diameter tension infiltrometer used to supply infiltrating water under suctions of 0, 0.5, 1, and 1.5 kPa. We consistently observed a lack of clear sorptivity-driven infiltration behaviour for all lysimeters under all surface-imposed suctions. Having ruled out artefacts of the tension infiltrometer–lysimeter system, surface seal development, air confinement, and a limited 'infiltration capacity' of the soil's top 50 mm layer, we conclude that direct and indirect effects of weak hydrophobicity and air encapsulation are the most important controls. Hydrophobicity, which appears to restrict the first 5–10 mm of infiltration, occurs despite the soils being close to field capacity. During unsaturated infiltration some macropores are non-fillable to infiltrating water, and we suggest that these pores may also act to isolate parts of the pore network that could otherwise exhibit sorptivity, and thus restrict early-time infiltration. The interaction between hydrophobicity and the "non-fillable" pore network may be an important mechanism causing non-uniform infiltration through preferential flowpaths. This may enhance air encapsulation by effectively blocking the escape path for the displaced air from parts of the pore network, further restricting the expression of sorptivity. In this sense the early-time infiltration behaviour of this soil is seen to be governed by the dynamic interaction between sorptivity, hydrophobicity, the network of air-filled pores, preferential flow and air encapsulation.

1. Introduction

Infiltration characteristics of the soil surface determine whether irrigation or rainwater moves to surface water as runoff, infiltrates into soil storage, or contributes drainage to groundwater. Likewise, infiltration is a key process determining the degree to which contaminants interact with the soil's filtering and buffering capability. The efficient use of water for agricultural crops and effective protection of fresh water from contamination could be greatly enhanced by a better understanding of infiltration dynamics.

All infiltration models share the common feature that the infiltration rate (i_t) is higher when water first enters the soil and then decreases (Jury and Horton, 2004). The commonest model is the two-parameter equation of Phillip (1957)

$$I = S\sqrt{t} + At, \tag{1}$$

where I (L) is cumulative infiltration, S ($L\,T^{-1/2}$) the soil sorptivity (a function of the supply water potential Ψ_{TI} and the antecedent soil matric potential Ψ_i), t is time, and A ($L\,T^{-1}$) is a parameter related to the soil's hydraulic conductivity. At early times the first term of Eq. (1) is dominant, as the air-filled portion of the pore network exerts sufficient capillary forces (via the matric potential, Ψ_m) to cause rapid imbibition of water at the soil surface.

Numerous examples in the literature show that infiltration can be explained by the Philip equation, with a number of researchers using the tension infiltrometer to study the S relationship at near-saturation (Angulo-Jaramillo et al., 1997; Clothier and Smettem, 1990; Sauer et al., 1990; Thony et al., 1991). Accurate measurement of the $S(\Psi_{TI}, \Psi_i)$ relationship for the surface layer is critical for understanding the

* Corresponding author. Tel.: +64 3 321 9663; fax: +64 3 321 9989.
E-mail address: carricks@landcareresearch.co.nz (S. Carrick).

0016-7061/$ – see front matter © 2010 Elsevier B.V. All rights reserved.
doi:10.1016/j.geoderma.2010.11.006

dynamics of soil water in response to rainfall or irrigation, particularly because it is the norm in many agricultural soils for the rate of rainfall or irrigation to be less than the saturated soil infiltration rate (Jarvis, 2007). The short time required to measure S is also seen as more practical than waiting for steady-state conditions, and has resulted in a number of methods being developed to estimate other important hydraulic attributes from the S relationship such as hydraulic conductivity, $K(\Psi_m)$, the characteristic mean pore size, λ_m, the sorptive number α^*, and the flux potential Φ (Reynolds and Topp, 2008).

In a series of tension infiltrometer experiments on large lysimeters we carried out, early-time infiltration often started slowly and increased with time, the inverse of Eq. (1). This atypical behaviour raises the possibility that features of our tension infiltrometer system may have influenced infiltration behaviour and generated artefacts in measured hydraulic attributes, or that some other process was suppressing the influence of capillarity. The aim of this paper is to examine the evidence for mechanisms, outside of sorptivity, dominating early-time infiltration and identify the most likely mechanisms and their interactions.

2. Materials and methods

2.1. Soil description

The sampling location was on the Canterbury Plains, South Island, New Zealand (43°33′ S, 171°38′ E). The soil is a well-drained silt loam (26% clay, 9% sand) Dystric Cambisol, formed into ca. 1 m of loess overlying stony river alluvium, and under rainfall of ca. 930 mm yr^{-1}. The site had been under grazed pasture for about 20 years. Our field morphological description revealed a 200-mm-thick topsoil (A horizon) with strongly developed very fine to fine subangular blocky structure. We later identified a surface layer (0–50 mm depth), which compared to the rest of the topsoil had higher organic carbon (3.6–3.9% vs. 2.6–3%), lower bulk density (1.02–1.07 vs. 1.20–1.28 g cm^{-3}), and higher total porosity (59–61% vs. 52–55%).

2.2. Lysimeter extraction and instrumentation

We collected four lysimeters (500-mm diameter, 700-mm height) according to the method of Cameron et al. (1992). In short, lysimeters were collected by digging a cylindrical pedestal of soil and gradually fitting the lysimeter casing down over the pedestal. This was finished when the lysimeter was 750-mm deep, as the last 50-mm of soil was later removed and replaced with sandy gravel to re-create free-draining conditions found at this depth in the field. The lysimeter casing has a 5-mm-thick internal cutting ring, which acts to carve the undisturbed lysimeter monolith from the soil pedestal as the casing is gently pushed downwards. This leaves a 5-mm gap between the lysimeter casing and the monolith which is then sealed by insertion of molten petrolatum. When it cools and solidifies the petrolatum prevents any edge-flow down the lysimeter wall during infiltration experiments (Cameron et al., 1992). A cutting plate was then used to remove the lysimeter monolith from the underlying soil, after which it was fixed to the lysimeter base so it could then be lifted out of the ground and transported back on an air-cushioned trailer to the laboratory.

Full details of the experimental set-up are provided in Carrick (2009). Tensiometers and CS616 water content reflectometers (WCR) were installed horizontally at layer boundaries (20, 200, 400, and 600-mm). Tensiometers were installed in an evenly spaced radial pattern around the lysimeter, with each ceramic cup located 100 mm into the soil. The tensiometers were constructed from 9.5-mm-diameter by 28.5-mm-long ceramic cups, and differential pressure transducers that were individually calibrated for both water pressure and temperature fluctuations. A CR1000 datalogger (Campbell Scientific Inc., Utah, USA) recorded sensor measurements every minute. Only data from sensors at 20 mm depth are presented here, because the focus is on early-time infiltration. The tensiometer response at all depths, the long-time infiltration behaviour, and derivation of hydraulic conductivities is presented in Carrick et al. (2010). The number of sensors at 20 mm depth varied among the lysimeters: lysimeters one and three (L1, L3) had one WCR and seven tensiometers; Lysimeter 2 (L2) had one WCR and four tensiometers. Lysimeter 6 (L6) had one WCR but no tensiometers, as this was the first lysimeter studied and the importance of the 0–50 mm layer was not initially recognised. Infiltration data from L6 are presented only to demonstrate the consistency among the lysimeters.

2.3. Lysimeter infiltration experiments

Water was applied with a 480-mm-diameter tension infiltrometer at surface-imposed suctions of 0, 0.5, 1 and 1.5 kPa in four separate experiments for each lysimeter. Drainage at the lysimeter base was under a suction equal to that applied to the surface, established by a vacuum pump pulling air through a bubble tower, which was set to apply the same suction as the lysimeter top. Between experiments the infiltrometer was removed and lysimeters were allowed to drain down to achieve a similar antecedent condition, as indicated by measurements of Ψ_m (i.e. −5 to −10 kPa in the topsoil, and −4 to −6 kPa in the subsoil). The datalogger recorded every millimetre of cumulative infiltration, calculated from the output of a pressure transducer installed at the base of the infiltrometer water reservoir. Full details of the experimental set-up are provided in Carrick (2009).

Before conducting the series of experiments on each lysimeter, we carefully removed pasture foliage. Generally, the soil surface was relatively level and was left undisturbed, although any large undulations greater than ca. 20 mm high were removed by using a knife to carefully pick the surface. The picking generally dislodged intact aggregates and no obvious smearing or pore blockage occurred. Next, we laid a 90 μm nylon retaining membrane on the soil surface, followed by a 10-mm-thick layer of fine (250–106 μm) glass bead contact material (Spheriglass, no. 2227, Potters Industries Ltd) in order to ensure good contact between the soil and infiltrometer (Reynolds, 2006, 2008; Reynolds and Zebchuk, 1996). The nylon retaining membrane served to prevent the contact material blocking soil pores.

The infiltrometer water reservoir was filled with a solution of tap water (equivalent to untreated irrigation water), 0.005 M $CaSO_4$, and thymol (0.5 g l^{-1}) to promote aggregate stability and inhibit biological activity (McKenzie and Cresswell, 2002; Skaggs et al., 2002). To minimise the effect of temperature fluctuations on infiltration, the lysimeter experiments were conducted indoors.

2.4. Estimation of soil sorptivity

The influence of capillarity on early-time infiltration is usually studied by fitting Eq. (1) to cumulative infiltration data, to estimate a value of the soil sorptivity, S (Minasny and McBratney, 2000). The most common method assumes that over some initial phase of infiltration capillarity dominates all other forces, and therefore

$$I = S\sqrt{t}, \tag{2}$$

such that a plot of I against $\sqrt{t}$ produces a straight line with zero intercept and slope equal to S (Cook, 2008; Minasny and McBratney, 2000). It is well recognised, however, that initial infiltration into the contact layer of a tension infiltrometer offsets the actual start time of soil infiltration (t_0). This in turn makes it difficult to determine the later time when gravity starts to significantly influence infiltration, and when Eq. (2) is no longer applicable (Clothier, 2001; Cook, 2008;

Minasny and McBratney, 2000). Cook (2008) recommends a better method to identify t_0 is to follow Smiles and Knight (1976) and perform a square-root-of-time transformation on cumulative infiltration:

$$\frac{I}{\sqrt{t}} = S + A\sqrt{t}. \quad (3)$$

when $I\sqrt{t}$ is plotted against $\sqrt{t}$ a non-linear initial section, attributed to the effects of the contact material, is followed by a linear section, the intercept of which is equal to S. This section has zero slope if capillarity is the sole mechanism for infiltration (Cook, 2008).

2.5. Measurement of hydrophobicity

We quantified soil hydrophobicity using the repellency index (RI) (Tillman et al., 1989), which is based on the ratio of water sorptivity (S_w) to the sorptivity of ethanol (S_e). Ethanol provides a reference liquid unaffected by hydrophobicity, owing to its zero contact-angle with solid surfaces. In a non-hydrophobic soil this ratio is 1.95 so that the RI is calculated as

$$\mathrm{RI} = 1.95(S_e / S_w), \quad (4)$$

where RI>1.0 for hydrophobic soils.

The main advantage of this method is that it enables quantification of hydrophobicity on infiltration for undisturbed soils at any antecedent water content, compared to the water-drop penetration test, which is only sensitive to severe hydrophobicity that may only become apparent at low water contents (Jarvis et al. 2008). After the lysimeter experiments, we extracted three small cores (100-mm diameter, 50 mm deep) from the surface layer of L1 and equilibrated them on a tension table to −8 kPa, which was the same antecedent Ψ_m measured for the equivalent lysimeter-scale infiltration experiment (i.e. L1 0.5 kPa). Infiltration of water and ethanol was measured during separate experiments for each core, where a 100-mm tension infiltrometer supplied the infiltrating solution under a surface suction of 0.4 kPa, with the same suction applied to the base of the core. As with the lysimeter-scale experiments, a nylon membrane and thin (2–3 mm) layer of glass beads was used to ensure good contact with the infiltrometer. For each core the water infiltration experiment was conducted first, before the core was returned to the tension table to re-equilibrate to −8 kPa, and then the ethanol infiltration experiment was conducted. Hydrophobicity experiments were not conducted on the other lysimeters, because they had been previously dissected for characterisation of physical and chemical analysis, before we became aware of the possible influence of hydrophobicity on our early-time infiltration behaviour.

2.6. Estimating the infiltration capacity

We define an "antecedent infiltration capacity" (I_c) as the depth (mm) of infiltrating water required to wet the top 50-mm layer of soil, from the antecedent matric potential, Ψ_i, to the "target" Ψ_m set by the suction of the tension infiltrometer:

$$I_c = 50[\theta_v(\psi_m) - \theta_v(\psi_i)]. \quad (5)$$

Here $\theta_v(\Psi_m)$ is the volumetric water content at the "target" Ψ_m set by the tension infiltrometer, based on the water-release characteristic of three small cores sampled from 0–50 mm depth of each lysimeter, following the infiltration experiments. $\theta_v(\Psi_i)$ is the volumetric water content at the antecedent matric potential (measured by the *in situ* tensiometers immediately prior to the start of infiltration). We make two estimates of I_c, comparing $\theta_v(\Psi_i)$ based on using the θ_v value measured from the *in situ* WCR immediately prior to the start of infiltration, or alternately estimating $\theta_v(\Psi_i)$ from the water-release characteristic of the small cores.

The magnitude of I_c is particularly important in determining the range of I over which sorptivity can be expected to drive infiltration. We calculate I_c for the 0–50 mm depth, largely because this depth coincides with the location of both the *in situ* WCR and tensiometers, as well as the small cores used to measure the soil water characteristic. Clothier and Smettem (1990) also identify that steady-state infiltration can be expected once the wetting front has penetrated 50–100 mm depth.

2.7. Estimating air-filled porosity

We estimated changes in the air-filled porosity (ε_a) during infiltration as,

$$\varepsilon_a = \varepsilon_t - \theta_v, \quad (6)$$

where ε_t is the total porosity measured from the three small cores sampled from each lysimeter, and θ_v is the temporally varying volumetric water content measured by the *in situ* WCR.

3. Results and discussion

The first two sections present the early-time results of the lysimeter infiltration experiments and the attempt to derive sorptivity values. This was the original objective of the project, but as shown below we could not obtain reliable sorptivity values. The subsequent sections present the results of the investigation into mechanisms that may have impeded sorptivity.

3.1. Measurement of infiltration rate, under different surface-imposed suctions

Fig. 1 shows the effect of controlling surface suction on infiltration rate (i_t). Clearly the infiltration behaviour does not follow Eq. (1), which predicts a transient phase with higher i_t, followed by a decline to a steady-state value. These results do have a transient phase, but i_t more typically increases initially (e.g. L3 0, 0.5 and 1 kPa). The only experiment where i_t decreases during the transient phase is L6 0 kPa, and even then not strictly consistent with $t^{1/2}$ behaviour.

The early-time behaviour is revealed more clearly using infiltration rates calculated over 1-mm cumulative infiltration intervals for the first 20 mm (Fig. 2). An initially higher i_t is apparent during the first 3–4 mm of saturated infiltration for L2, L3 and L6, and also is apparent during the first 1–3 mm of unsaturated infiltration into L2 and L6 (e.g. L2 0.5 and 1 kPa). However, these data also show a pattern in which an initial sharp decline in i_t is followed by a steady increase. The remaining experiments of L1 and L3 show a contrasting infiltration pattern, where i_t starts slowly and then steadily increases. In some experiments i_t fluctuates, with no clear overall pattern (e.g. L3 1 and 1.5 kPa). The only experiment consistent with the Philip model is L2 1.5 kPa, where i_t starts at 10 mm h^{-1}, and then steadily declines to 0.1–0.2 mm h^{-1} by 6 mm of cumulative infiltration.

3.2. Estimation of soil sorptivity

Fig. 3 shows that it is not possible to use Eq. (2) to describe the early-time infiltration behaviour in this study, where it is difficult to identify discrete linear portions of the graph from which S can be derived. The inappropriateness of our data to this kind of analysis is confirmed when we apply the approach of Smiles and Knight (1976) (Fig. 4). It is difficult to consistently identify clear periods when capillarity is the dominant mechanism. Under saturated infiltration, fitting of Eq. (3) to the early-time linear plot may be suitable for L2, L3 and L6, but would produce negative values of S for L1. There are some unsaturated experiments where fitting of Eq. (3) would produce credible estimates of S (e.g. L2 and L6 1.5 kPa), but most experiments

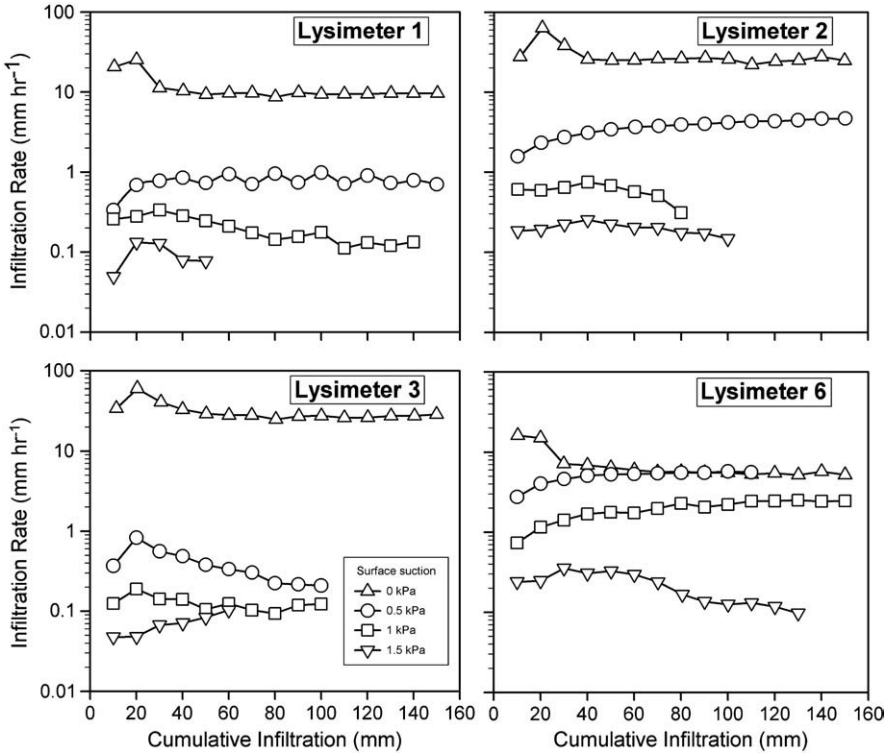

Fig. 1. Infiltration rates for four lysimeters calculated over 10-mm cumulative infiltration intervals under controlled surface suctions of 0, 0.5, 1 and 1.5 kPa.

show an apparent negative S (e.g. L1 and L3 0.5 kPa), or no clear linear behaviour (e.g. L3 1 and 1.5 kPa). These results suggest that Eq. (1) does not provide an adequate explanation of infiltration into this particular soil and under the boundary conditions of our experiments (Smiles and Knight, 1976).

The Smiles and Knight (1976) method makes it clear also that even where rapid early infiltration occurred, it may not be solely the result of sorptivity. This is illustrated by the L2 1.5 kPa experiment, where the rapid early-time infiltration (Fig. 2) results from 2 mm of infiltration that was necessary to wet the contact material (Fig. 4).

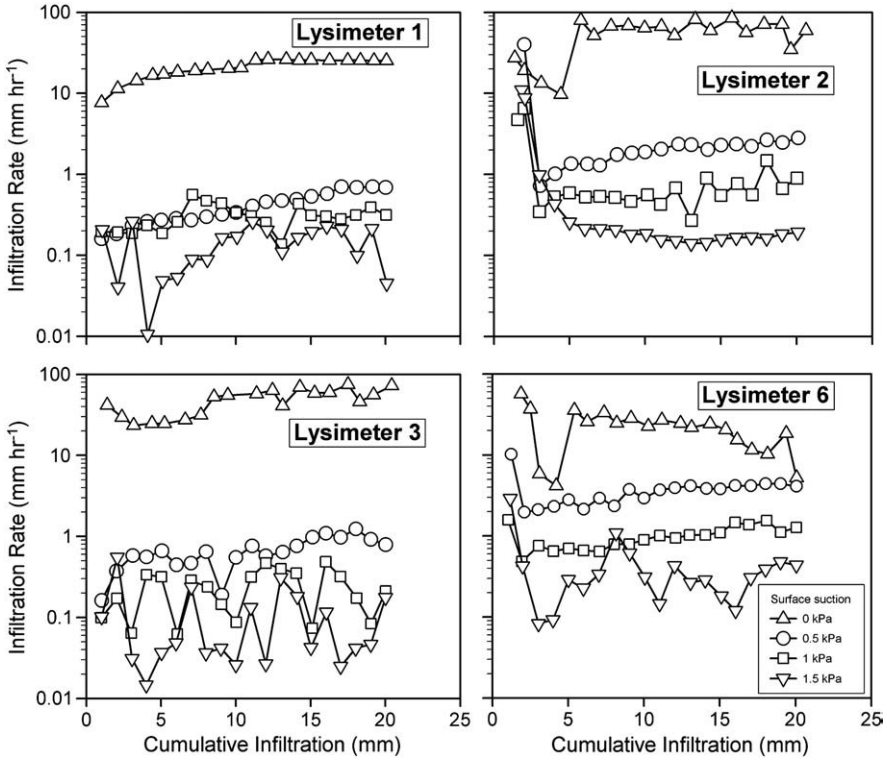

Fig. 2. Infiltration rates of four lysimeters during the transient phase of infiltration, where infiltration occurs under controlled surface suctions of 0, 0.5, 1 and 1.5 kPa. The transient phase is assumed to occur within the first 20 mm of cumulative infiltration.

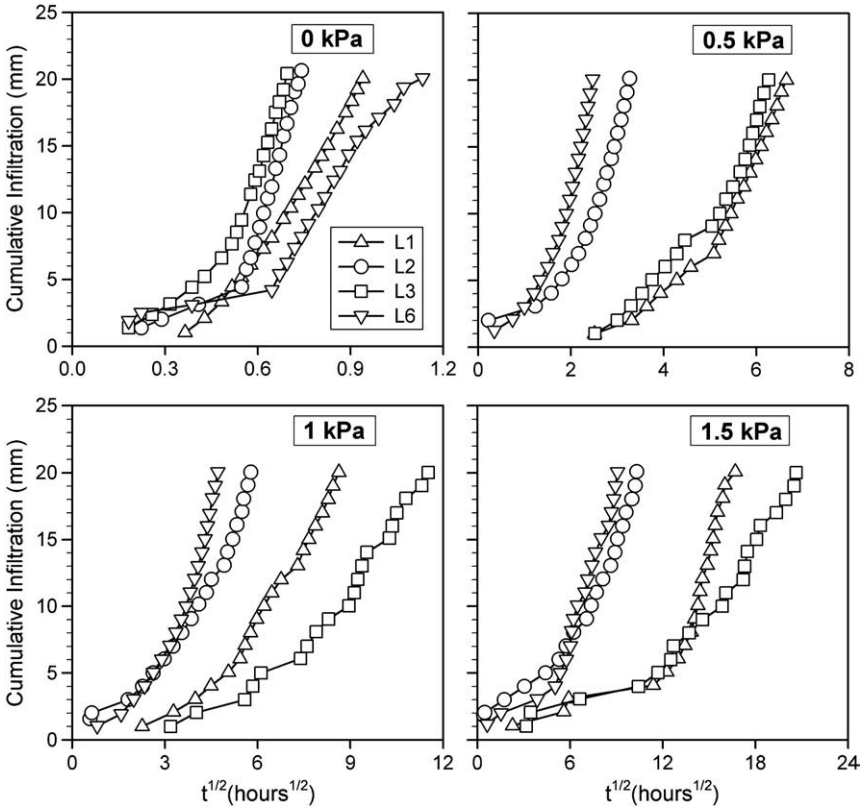

Fig. 3. Cumulative infiltration versus square-root of time ($t^{1/2}$) for four lysimeters, during early-time infiltration under surface-imposed suctions of 0, 0.5, 1, and 1.5 kPa.

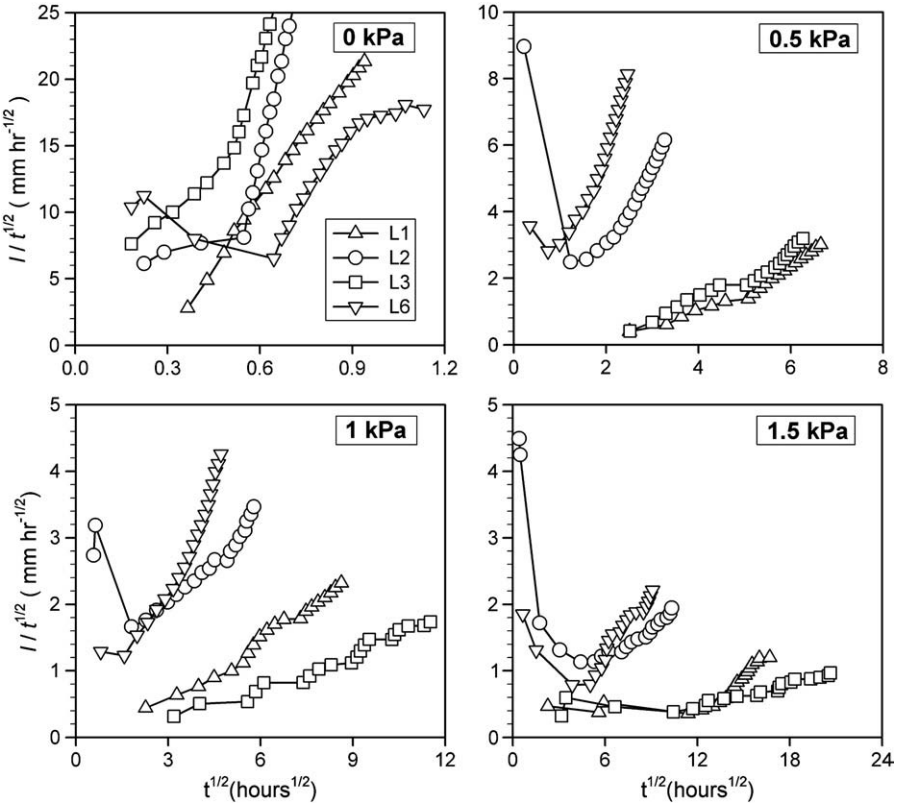

Fig. 4. Plot of square-root-of-time transformed cumulative infiltration ($I/t^{1/2}$) versus square-root of time ($t^{1/2}$) for four lysimeters, during early-time infiltration under surface-imposed suctions of 0, 0.5, 1, and 1.5 kPa.

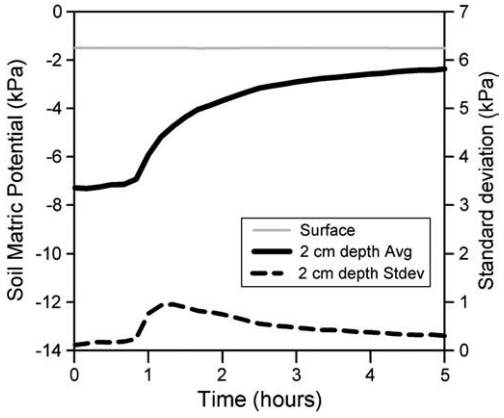

Fig. 5. Response of tensiometers at 20 mm depth of Lysimeter 2, after infiltration was initiated under a surface suction of 1.5 kPa.

Measurements of Ψ_m at 20 mm depth (Fig. 5) show that although 2 mm of cumulative infiltration had occurred within the first 15 min, this water did not wet the 20 mm depth for least another 50 min. If the infiltrating water had immediately entered the soil there should have been a clear Ψ_m response, because 2 mm of infiltration is 30–50% of the estimated antecedent infiltration capacity for the 0–50 mm layer (Table 1).

3.3. Possible restrictions of the tension infiltrometer on sorptivity

The tension infiltrometer's design should not cause a flow rate restriction. Potentially the rate-limiting factor is the hydraulic conductivity of the contact material (K_{cs}), but the measured i_t were <100 mm h^{-1}, well below the reported K_{cs} of 410 to 264 mm h^{-1} for the suctions applied in our experiments (Bagarello et al., 2001; Reynolds, 2006; Reynolds and Zebchuk, 1996). Generally the contact material will also exhibit a high S, especially when dry, which will accelerate early-time infiltration and result in overestimation of S compared with the true soil S (Minasny and McBratney, 2000).

Minasny and McBratney (2000) carried out a rigorous analysis of the effect of contact material on five methods used to estimate S from early-time unsaturated infiltration. The effect was modelled using a numerical simulation of infiltration into a loam and a clay, as well as field-tested on heavy clay. The experiments showed that all methods overestimated S when contact material was used. In the field experiment, the overestimation persisted even after the effect of the initial contact material wetting was eliminated from the infiltration data. The consistently higher S was attributed to better contact with the soil surface. In contrast to the findings of Minasny and McBratney (2000), we identify restricted sorptive behaviour, and therefore the contact material is not likely to be the impeding factor.

However, in our experiments a retaining membrane was used between the contact material and the soil surface, and it is possible that air gaps at the interface interrupted infiltration, particularly at the higher suctions. The likelihood of poor contact is explored in Fig. 6, which shows that installation of the contact material onto the retaining membrane resulted in an immediate response in the tensiometers at 20 mm depth. The variability between tensiometers also decreased immediately, indicating a uniform wetting of the surface layer, even when the initial Ψ_m of the beads was -1 to -1.5 kPa, and gaps greater than 0.2–0.3 mm between the soil and the retaining membrane would restrict response from areas of the soil.

Furthermore, the presence of slow early-time infiltration in the saturated infiltration experiments indicates that poor contact is not the governing mechanism, as gaps between the contact material and the soil surface would not restrict infiltration.

3.4. The possibility of blockage of surface-connected soil pores

A surface seal or crust blocking surface pores is known to impede infiltration. Surface seal development can be caused by deposition of fine particles by surface runoff, by dispersion caused by a high percentage of exchangeable sodium, or by soil collapse due to encapsulated air and weak aggregate strength caused by low clay, organic matter, and iron–aluminium oxides (Hillel, 1998; Marshall et al., 1996). Schwarzel and Punzel (2007) argued that a surface seal formed by surface preparation and installation of contact material resulted in lower infiltration rates measured under a tension infiltrometer than under a hood infiltrometer.

In this study we do not see infiltration behaviour typical of a surface seal; at early-time i_t often starts slowly, then increases (Fig. 2). Nor is the soil likely to form a surface seal under the prevailing conditions. Care was taken to not disturb the soil surface when vegetation was removed, and a membrane was placed on the surface to prevent blocking of soil pores by the contact material. The soils are likely to have low exchangeable sodium levels, and a wet-sieve stability test indicated ca. 80% aggregate stability in the topsoil, reflecting the moderate clay and organic matter contents (Carrick, 2009). A 0.005 M $CaSO_4$ infiltrating solution was used to further promote aggregate stability. Surface seals tend to form under raindrop impact (Hillel, 1998; Marshall et al., 1996) whereas wetting from the tension infiltrometer has very low kinetic energy, particularly under unsaturated infiltration.

Air encapsulation did occur during early-time infiltration (refer to Section 3.7), but a separate slaking test showed individual aggregates to be stable during rapid saturation, and therefore we consider encapsulated air to have caused negligible aggregate breakdown.

3.5. The effect of antecedent soil wetness on sorptivity

The antecedent water content (θ_i) at the start of infiltration is a critical determinant of early-time infiltration, particularly with

Table 1
Antecedent matric potential (Ψ_i) and infiltration capacity (I_c)[a] for the 0–50 mm depth of each lysimeter (1–3), prior to infiltration under different surface suctions.

Surface suction kPa	L1			L2			L3		
	Ψ_i (kPa)[b]	*WCR* I_c (mm)[c]	*Core* I_c (mm)[d]	Ψ_i (kPa)	*WCR* I_c (mm)	*Core* I_c (mm)	Ψ_i (kPa)	*WCR* I_c (mm)	*Core* I_c (mm)
0	−8.4	9	7	−5.1	9	9	−9.0	11	7
0.5	−8.2	6	5	−5.3	6	5	−8.9	7	4
1	−6.3	6	4	−7.1	10	5	−7.0	9	4
1.5	−6.2	7	4	−7.3	7	4	−8.4	8	4

[a] Two estimates of I_c are provided, from: A. *In situ* water content reflectometers (WCR I_c); B. Water-release data from three small cores sampled from each lysimeter (Core I_c).
[b] The standard error of Ψ_i was 0.1–0.4 kPa.
[c] The accuracy of the WCR is ± 1.5 mm.
[d] The standard error of the core I_c was 0.3–0.5 mm.

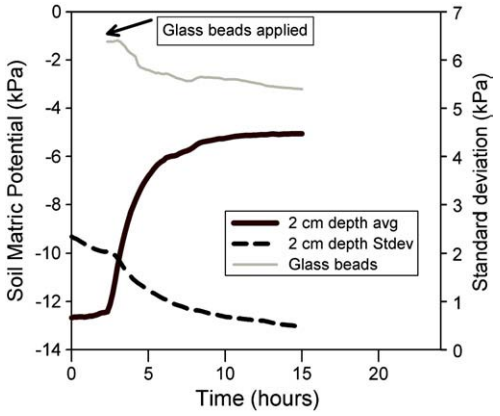

Fig. 6. Response of tensiometers at 20 mm depth of Lysimeter 1, when just moist glass beads (~20 mm deep) were placed on the surface, but the tension infiltrometer was not installed. Any gaps greater than ~0.2–0.3 mm between the glass beads and the soil surface would have restricted wetting of the surface soil layer, as well as further restriction by smaller gaps as the Ψ_m in the beads decreased.

respect to the influence that the soil's capillarity (sorptivity) exerts on the infiltrating water. Sorptivity tends to decrease with increasing θ_i, because both the matric potential gradient and the available water storage capacity decreases (Reynolds and Topp, 2008). Reynolds (2008) recommends that the antecedent matric potential (Ψ_i) should be ≤ -5 to -10 kPa to ensure sufficient matric potential gradient. Kumke and Mullins (1997) observed an exponential relationship between S and Ψ_i, where S increased rapidly below about -6 kPa, although S still increased between two and seven times as Ψ_i decreased from -2 to -6 kPa. For this study the Ψ_i for each experiment ranged from -5.1 to -9 kPa (Table 1), which was the quasi-steady state achieved after 7–10 days' drainage from the previous experiment. This was interpreted as 'field capacity' during the winter drainage season, and thus a relevant Ψ_i for these experiments.

A useful approach is to express $\theta_i(\Psi_i)$ in terms of the antecedent infiltration capacity (I_c), where I_c is the depth (mm) of infiltrating water required to wet the 0–50 mm layer from Ψ_i to the "target" Ψ_m, set by the tension infiltrometer. Table 1 estimates I_c based on either the θ_i measurement of the *in situ* water content reflectometer (WCR), or the water-release characteristic of three small cores sub-sampled from each lysimeter.

The WCR indicates a higher I_c than that estimated from the small cores. The difference may be partly explained by the WCR accuracy ($\pm 3\%$), although in a number of experiments the differences are larger than the WCR error alone. The higher WCR estimate of I_c WCR may also indicate encapsulated air, which is likely to be less in the small cores that were saturated for one week prior to measurement. The differences may also reflect the larger sample volume of the soil cores (1180 cm^3), compared with sensing volumes of 338 cm^3 (Logsdon and Hornbuckle, 2006) and 79.2 cm^3 (Blonquist et al., 2005) estimated for the WCR, on the basis of radii of 13 and 6.5 mm around each wave guide.

Table 1 indicates that I_c was at least 4 mm prior to unsaturated infiltration, and at least 7 mm prior to saturated infiltration. Therefore, sorptivity behaviour should have been observed for at least these depths of infiltration, assuming that 0–50 mm is the soil depth controlling the sorptivity stage, and that the contact material absorbs none of the infiltrating water. As discussed earlier, the contact material likely absorbed some of the infiltrating water, which would increase the amount of cumulative infiltration over which sorptivity behaviour should be dominant. Based on these I_c values we conclude that the antecedent wetness is not limiting sorptivity-driven infiltration.

3.6. The effect of hydrophobicity on sorptivity

Wallis et al. (1991) showed that hydrophobicity is potentially widespread in New Zealand soils, although the antecedent water contents (θ_i) of the soils in their analysis were considerably less than the θ_i of this study. Generally, hydrophobicity is associated with dry soils, and it is thought that there is a critical moisture content above which hydrophobicity disappears (Dekker et al., 2001). In a survey of 41 common UK soil and land use types, Doerr et al. (2006) showed hydrophobicity to be virtually absent for $\theta_i > 28\%$ using the waterdrop penetration test, however this approach is only sensitive to severe hydrophobicity and may not detect sub-critical hydrophobicity (Jarvis et al., 2008). Strong sub-critical hydrophobicity has been observed by Clothier et al. (2000) for a NZ (Ramihi) soil where θ_i was $\approx 40\%$, and by Jarvis et al. (2008) when θ_i was 36%, when using a tension infiltrometer to compare the infiltration of water and ethanol. These antecedent water contents are similar to those of the present study where θ_i was 30–50%. Clothier et al. (2000) observed that hydrophobicity in the Ramiha soil kept the infiltration rate (i_t) low for about 100 min, before it increased rapidly to a steady rate ca. 5 times greater. This infiltration pattern is similar to that observed during a number of our experiments, and indicates that hydrophobicity may be a mechanism influencing early-time infiltration.

We confirmed that hydrophobicity was present during early-time infiltration in this study, using sorptivity data derived from ethanol and water infiltration experiments on small cores (Fig. 7). These data provided an average repellency index of 6.8, where values greater than unity show the presence of hydrophobicity (Tillman et al., 1989).

In a review of this paper, it was suggested that the hydrophobic behaviour may be a measurement artefact, induced through the use of thymol biocide in the infiltrating solution. Thymol has low water solubility, and evidence of hydrophobic properties has been shown in the medical literature (Braga et al., 2006). A review of the literature

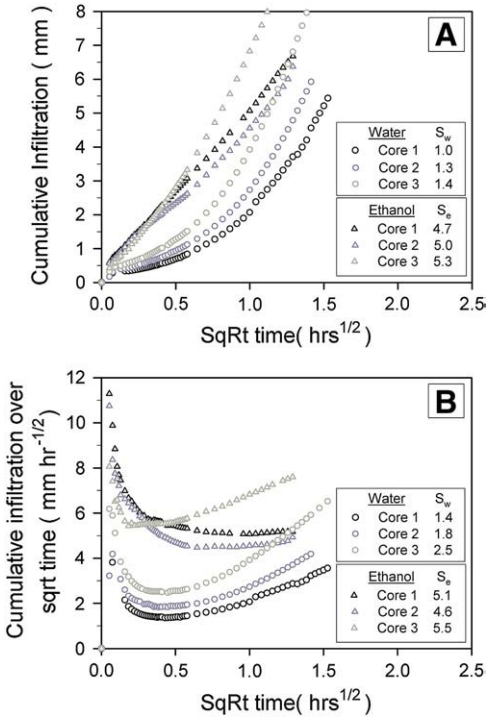

Fig. 7. Early-time infiltration of water and ethanol into three small cores sampled from the 0–50 mm depth of Lysimeter 1 plotted as: A. cumulative infiltration versus $t^{1/2}$, and B. as square-root-of-time transformed cumulative infiltration ($I/t^{1/2}$) versus square-root of time ($t^{1/2}$). Sorptivity of water (S_w) and ethanol (S_e) are estimated from the slope of the early-time linear segments in A and from the intercept of the segment of the plot with zero slope in B.

found no studies that link thymol with the development of soil hydrophobicity, although thymol has been previously used in hydrophobicity research (Chan 1992; Regalado and Ritter, 2005). Importantly, Chan (1992) found that thymol was an effective means to *reduce* the development of hydrophobicity. Our hydrophobicity tests were also conducted using thymol-free water. However, the cores were sampled from a lysimeter where thymol had been used, but there was at least one month between experiments which should have been sufficient time for the thymol in the soil to break down, given its dissipation half life of 5 days in soil (Hu and Coats 2008). Further, if thymol did induce hydrophobicity it does not explain why in some experiments a clear sorptivity phase commenced after 5–10 mm infiltration, even though the infiltrating solution still contained thymol (0 kPa experiments, Fig. 3). Based on this evidence we argue that the hydrophobicity was unlikely to be an artefact of our measurement method, although we recommend that future research should determine the effects of thymol on infiltration, given thymol's use is recommended as a standard measurement method (McKenzie and Cresswell, 2002; Skaggs et al., 2002).

3.7. The effect of air encapsulation on sorptivity

Infiltration is effectively a two-phase flow system, where infiltrating water also displaces pore air (Faybishenko, 1999; Hillel, 1998). Generally it is thought that this displacement occurs readily, and therefore infiltration only needs to be studied purely in terms of the water phase dynamics. However, studies have shown that the air phase can have a large influence on infiltration, either as confined air ahead of the wetting front, or as encapsulated air bubbles in the transmission zone (Constantz et al., 1988; Faybishenko, 1999; Wang et al., 1998). Air encapsulation is thought to occur because of variation in pore water velocity, meaning some pore spaces fill before others (Constantz et al., 1988). Air confinement has been observed in field soils with a high water table, or a slowly permeable subsoil that restricts the displacement of soil air (Fayer and Hillel, 1986; Hammecker et al., 2003; Navarro et al., 2008).

In the study of Faybishenko (1999) infiltration followed a three-stage pattern. This was attributed to the effects of air encapsulation that initially slowed infiltration, followed by an increase in i_t as mobile air is removed, before a reduction in i_t to a quasi-steady-state value. This pattern is similar to that observed during our experiments (Fig. 1), suggesting that air encapsulation may be a mechanism influencing early-time infiltration.

Under saturated infiltration, the slow early-time infiltration of all lysimeters coincided with high air-filled porosity (ε_a), with i_t increasing as ε_a decreased (Fig. 8). The relationship is particularly clear for L1 and L3, where ε_a was measured every minute and determined for 1-mm cumulative infiltration intervals. For L2 and L6 ε_a was only recorded as a 10-min average, although it still indicates a relationship between a low i_t and a high ε_a. However, the extent to which air encapsulation is a direct influence on infiltration is uncertain, as opposed to being an indirect effect of hydrophobicity. The rapid wetting after 5–10 mm of infiltration may represent the breakdown of hydrophobicity. Clothier et al. (2000) also observed that hydrophobicity appeared to break down by about 5 mm of infiltration.

During unsaturated infiltration, air-filled pores are an inherent component, particularly when using a tension infiltrometer to exclude macropores from infiltration. Some pores will remain air-filled because they have a water entry suction lower than that imposed by the tension infiltrometer, herein termed the "non-fillable" air-filled porosity (ε_{anf}). Other parts of the pore network may fill with infiltrating water, because their water entry suction exceeds that imposed by the infiltrometer. These "fillable" pores are those that provide the antecedent infiltration capacity (I_c).

Table 2 shows a comparison of I_c (expressed here as a percentage of soil volume) with the expected ε_{anf} of each experiment, assuming that the 0–50 mm depth wets as expected (i.e. Ψ_m would equal that imposed by the tension infiltrometer). These results indicate that

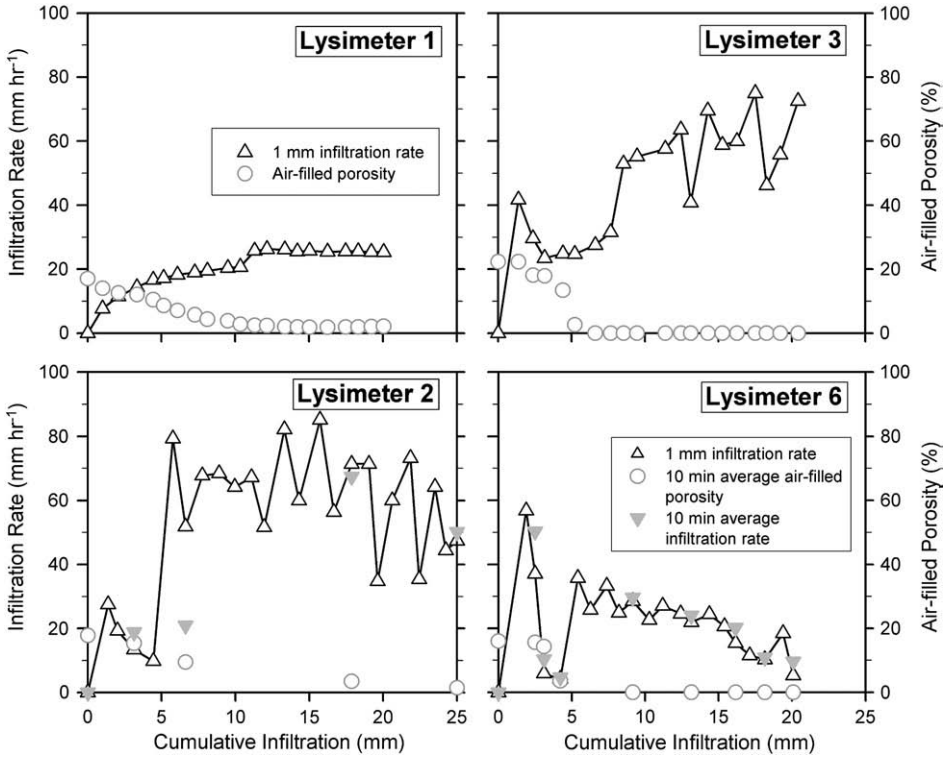

Fig. 8. Infiltration rate (i_t) and air-filled porosity (ε_a) of the 0–50 mm depth, for four lysimeters during saturated infiltration. The ε_a is calculated as the difference between the total porosity and water-filled porosity measured by the *in situ* WCR.

Table 2
Comparison of the non-fillable air-filled porosity (ε_{anf})[a] and the infiltration capacity (I_c, here expressed as a % by volume)[b] that could contribute to sorptivity-driven infiltration.

Surface suction (kPa)	L1				L2				L3			
	Ψ_i (kPa)	ε_{anf} (%)	*WCR* I_c (%)	*Core* I_c (%)	Ψ_i (kPa)	ε_{anf} (%)	*WCR* I_c (%)	*Core* I_c (%)	Ψ_i (kPa)	ε_{anf} (%)	*WCR* I_c (%)	*Core* I_c (%)
0	−8.4	0	17	14	−5.1	0	18	17	−9.0	0	22	15
0.5	−8.2	4	12	9	−5.3	8	11	9	−8.9	7	13	8
1	−6.3	5	12	8	−7.1	9	19	10	−7.0	7	19	7
1.5	−6.2	5	14	7	−7.3	10	14	8	−8.4	8	16	7

[a] The ε_{anf} is estimated from the small-core porosity relationships.
[b] Two estimates of I_c are provided, from: A. *In situ* water content reflectometers (WCR I_c); B. Water release from three small cores sampled from each lysimeter (Core I_c).

during unsaturated infiltration ε_{anf} is likely to be large proportionally to I_c. Assuming that both air- and water-filled components are interwoven in the pore network, it seems plausible that ε_{anf} could have a large restrictive influence on early-time infiltration, where the non-fillable pore network acts to isolate parts of the I_c network from the infiltrating water. The restricting effect of ε_{anf} will be enhanced if further air encapsulation occurs as infiltrating water fills the I_c component of the pore network.

Fig. 9 shows that air encapsulation is an important component of unsaturated infiltration. Under 0.5-kPa surface suction ε_a slowly declines towards the "target" ε_{anf} value, whereas under 1-kPa suction ε_a remains 9–14% above the "target" ε_{anf} value, meaning 40–60% of the I_c remains air-filled up to the first 20 mm of infiltration. This indicates that when infiltration occurs under a surface suction of >1 kPa, the air-filled macropores create a ε_{anf} network that has sufficiently large volume and interconnectedness to isolate large portions of the water-fillable pore network.

It is possible that the initial hydrophobicity and air-filled pore network interact to limit the infiltration pathways; hydrophobicity creates preferential flow, which in turn creates air encapsulation. Preferential flow is recognised as a mechanism that may lead to air encapsulation, where the variation in flow velocities may lead to parts of the pore network being unable to fill with water, because other water-filled pores have blocked air escape routes (Fayer and Hillel, 1986).

3.8. The effect of air confinement on sorptivity

It is possible that air confinement is also present, as an artefact of the tension infiltrometer and lysimeter system. The infiltrometer may block air escaping through the soil surface, and the lysimeter walls may block lateral air displacement. This effect has been observed in lysimeter studies by Wang et al. (1998), when air was not allowed to escape out of the base of a lysimeter.

In the air-confining situation of Wang et al. (1998) the soil air became compressed ahead of the wetting front until the air pressure was great enough to allow escape to the surface. Infiltration rate (i_t) was found to follow a "surging" pattern, inversely related to the rise and fall of the air pressure ahead of the wetting front. In the study of Fayer and Hillel (1986), infiltration at 137 mm h^{-1} resulted in soil air pressures increasing 0.5–1 kPa ahead of the wetting front, whereas Wang et al. (1998) measured increases of 1–5 kPa.

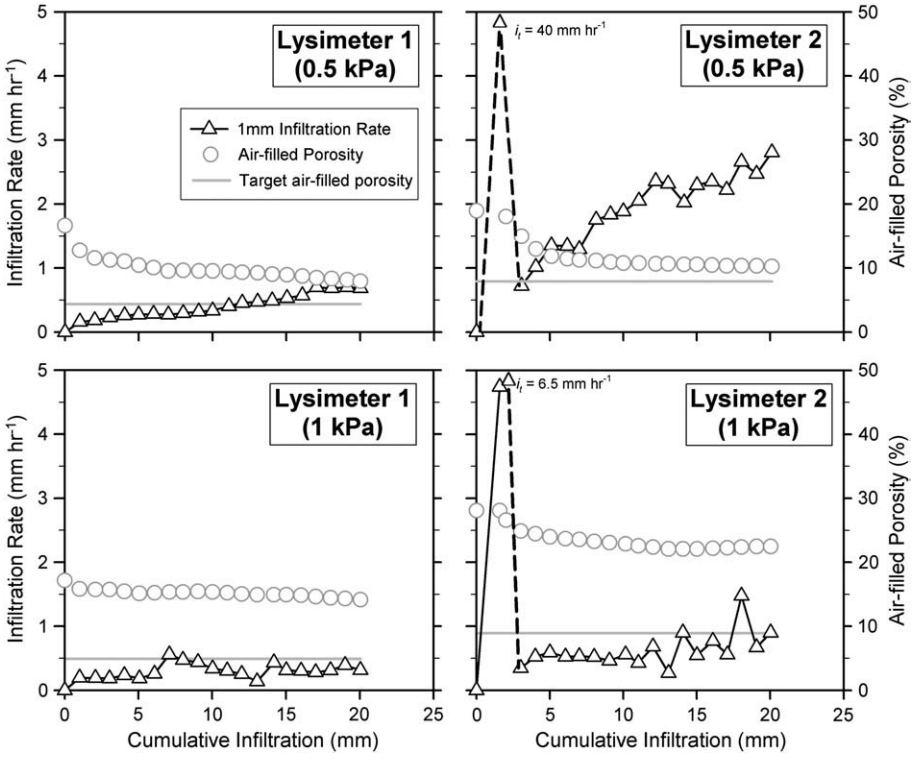

Fig. 9. Air-filled porosity (ε_a) for the 0–50 mm depth and infiltration rate (i_t) as unsaturated infiltration progresses, under surface suctions of 0.5 and 1 kPa. The "target" ε_a value is indicated, which is the value that ε_a should decline to (termed the non-fillable air-filled porosity, ε_{anf}) at the soil Ψ_m the soil should wet to, as set by the tension infiltrometer (i.e. Ψ_m of −0.5 or −1 kPa for the respective experiments).

Our experiments did not generally show a "surging" i_t during early-time infiltration, except during saturated infiltration into L2, L3 and L6 (Fig. 2). These lysimeters show an early stalling then rise in i_t that appears to be inversely related to the air-filled porosity (Fig. 8), which may reflect air confinement. However, the tensiometers at 200 mm depth remained steady during early-time infiltration, with no indication of an air-pressure spike prior to the arrival of the wetting front, indicating that the subsoil air permeability was adequate to cope with the displaced air.

During unsaturated infiltration, air compression is less likely to occur, because soil air should be able to be displaced into macropores. Importantly, it was difficult to maintain the applied drainage suction during early-time unsaturated infiltration. The drainage air-pumps needed to be on high, or additional pumps were required (L2 and L3), to cope with excess air that was draining through the lysimeters. Once the lysimeters had wet up, the drainage suction could be maintained by a single air-pump on low speed, and was often further restricted by a pipe clamp to reduce the bubble rate in the bubble tower. This further indicates that there was adequate subsoil air permeability.

4. Conclusions

Infiltration of water is commonly modelled by an equation that encapsulates rapid, sorptivity-driven early-time infiltration, which decays according to a $t^{-1/2}$ law toward a steady-state, gravity-driven infiltration rate Phillip (1957)). Our experiments showed non-typical infiltration into a silty Dystric Cambisol at or near field capacity, where water was supplied by a tension infiltrometer at suctions between 0 and 1.5 kPa. Infiltration often started slowly and then increased, before slowing to a steady phase. We conclude that weak hydrophobicity interacting with encapsulated air is the most likely combination of phenomena limiting early-time infiltration. Other possible mechanisms were ruled out, including: (i) artefacts engendered by the infiltrometer–lysimeter system, (ii) insufficient infiltration capacity of the soil prior to the experiments, (iii) surface seal development, and (iv) air confinement.

Hydrophobicity directly limits sorptivity in parts of the pore network and encourages preferential flow in others. Non-uniform infiltration then isolates parts of the pore network by air encapsulation and further limits sorptive behaviour. These effects are enhanced during unsaturated infiltration when non-fillable pores create volumes of the pore network that are inaccessible to infiltrating water. We also recommend that the potential effect of thymol inducing hydrophobicity needs further investigation, given that its use is currently recommended in standard methodology texts.

Acknowledgements

AgMardt funded this PhD project, with further support from Landcare Research, New Zealand, and the Centre for Soil and Environmental Quality, Lincoln University, Canterbury, New Zealand. We thank David Barlass for the use of his farmland.

References

Angulo-Jaramillo, R., Vandervaere, J.P., Roulier, S., Thony, J.L., Gaudet, J.P., Vauclin, M., 1997. Seasonal variation of hydraulic properties of soils measured using a tension disk infiltrometer. Soil Sci. Soc. Am. J. 61, 27–32.

Bagarello, V., Iovino, M., Tusa, G., 2001. Effect of contact material on tension infiltrometer measurements. Trans. ASAE 44, 911–916.

Blonquist Jr., J.M., Jones, S.B., Robinson, D.A., 2005. Standardizing characterization of electromagnetic water content sensors: Part 2. Evaluation of seven sensing systems. Vadose Zone J. 4, 1059–1069.

Braga, P.C., Dal Sasso, M., Culici, M., Bianchi, T., Bordoni, L., Marabini, L., 2006. Anti-inflammatory activity of thymol: inhibitory effect on the release of human neutrophil elastase. Pharmacology 77, 130–136.

Cameron, K.C., Smith, N.P., McLay, C.D.A., Fraser, P.M., McPherson, R.J., Harrison, D.F., Harbottle, P., 1992. Lysimeters without edge flow: an improved design and sampling procedure. Soil Sci. Soc. Am. J. 56, 1625–1628.

Carrick, S.T., 2009. The dynamic interplay of mechanisms governing infiltration into structured and layered soil columns. PhD thesis, Lincoln University, Canterbury, New Zealand. http://hdl.handle.net/10182/1328.

Carrick, S., Almond, P., Buchan, G., Smith, N., 2010. *In situ* characterization of hydraulic conductivities of individual soil profile layers during infiltration over long time periods. European Journal of Soil Science 61, 1056–1069. doi:10.1111/j.1365-2389.2010.01271.x.

Chan, K.Y., 1992. Development of seasonal water repellence under direct drilling. Soil Sci. Soc. Am. J. 56, 326–329.

Clothier, B.E., 2001. Infiltration. In: Smith, K.A., Mullins, C.E. (Eds.), Soil and Environmental Analysis: Physical Methods. Books in Soils, Plants, and the Environment. Marcel Dekker, New York, pp. 239–281.

Clothier, B.E., Smettem, K.R.J., 1990. Combining laboratory and field measurements to define the hydraulic properties of soil. Soil Sci. Soc. Am. J. 54, 299–304.

Clothier, B.E., Vogeler, I., Magesan, G.N., 2000. The breakdown of water repellency and solute transport through a hydrophobic soil. J. Hydrol. 231–232, 255–264.

Constantz, J., Herkelrath, W.N., Murphy, F., 1988. Air encapsulation during infiltration. Soil Sci. Soc. Am. J. 52, 10–16.

Cook, F.J., 2008. Unsaturated hydraulic properties: laboratory tension infiltrometer. In: Carter, M.R., Gregorich, E.G. (Eds.), Soil Sampling and Methods of Analysis. Canadian Society of Soil Science & CRC Press Boca Raton, FL, pp. 1075–1087.

Dekker, L.W., Doerr, S.H., Oostindie, K., Ziogas, A.K., Ritsema, C.J., 2001. Water repellency and critical soil water content in a dune sand. Soil Sci. Soc. Am. J. 65, 1667–1674.

Doerr, S.H., Shakesby, R.A., Dekker, L.W., Ritsema, C.J., 2006. Occurrence, prediction and hydrological effects of water repellency amongst major soil and land-use types in a humid temperate climate. Eur. J. Soil Sci. 57, 741–754.

Faybishenko, B., 1999. Comparison of laboratory and field methods for determining the quasi-saturated hydraulic conductivity of soils. In: Van Genuchten, M.T., Leij, F.J., Wu, L. (Eds.), Characterization and Measurement of the Hydraulic Properties of Unsaturated Porous Media: Proceedings of the International Workshop on Characterization and Measurement of the Hydraulic Properties of Unsaturated Porous Media, Riverside, California, 22–24 October 1997. University of California, Riverside, California, pp. 279–292.

Fayer, M.J., Hillel, D., 1986. Air encapsulation: I, Measurement in a field soil. Soil Sci. Soc. Am. J. 50, 568–572.

Hammecker, C., Antonino, A.C.D., Maeght, P., Boivin, J.L., 2003. Experimental and numerical study of water flow in soil under irrigation in northern Senegal: evidence of air entrapment. Eur. J. Soil Sci. 54, 491–503.

Hillel, D., 1998. Environmental Soil Physics. Academic Press, San Diego, CA. xxvii, 771 pp.

Hu, D., Coats, J., 2008. Evaluation of the environmental fate of thymol and phenethyl propionate in the laboratory. Pest Manage. Sci. 64, 775–779.

Jarvis, N.J., 2007. A review of non-equilibrium water flow and solute transport in soil macropores: principles, controlling factors and consequences for water quality. Eur. J. Soil Sci. 58, 523–546.

Jarvis, N., Etana, A., Stagnitti, F., 2008. Water repellency, near-saturated infiltration and preferential solute transport in a macroporous clay soil. Geoderma 143, 223–230.

Jury, W.A., Horton, R., 2004. Soil Physics. Wiley, Hoboken, N.J. xiv, 37 pp.

Kumke, T., Mullins, C.E., 1997. Field measurement of time to ponding. Soil Use Manage. 13, 24–28.

Logsdon, S.D., Hornbuckle, B.K., 2006. Soil moisture probes for a dispersive soil, TDR 2006. Purdue University, West Lafayette, USA, Sept. 2006. paper ID 13, https://engineering.purdue.edu/TDR/Papers, pp. 14.

Marshall, T.J., Holmes, J.W., Rose, C.W., 1996. Soil Physics. Cambridge University Press, Cambridge [England; New York. xiv, 453 p.

McKenzie, N.J., Cresswell, H.P., 2002. Selecting a method for hydraulic conductivity. In: McKenzie, N., Coughlan, K., Cresswell, H. (Eds.), Soil Physical Measurement and Interpretation for Land Evaluation. CSIRO, Collingwood, Australia, pp. 90–107.

Minasny, B., McBratney, A.B., 2000. Estimation of sorptivity from disc-permeameter measurements. Geoderma 95, 305–324.

Navarro, V., Yustres, A., Candel, M., García, B., 2008. Soil air compression in clays during flood irrigation. Eur. J. Soil Sci. 59, 799–806.

Phillip, J.R., 1957. The theory of infiltration. 4. Sorptivity and algebraic infiltration equations. Soil Sci. 84, 257–264.

Regalado, C.M., Ritter, A., 2005. Characterizing water dependent soil repellency with minimal parameter requirement. Soil Sci. Soc. Am. J. 69, 1955–1966.

Reynolds, W.D., 2006. Tension infiltrometer measurements: implications of pressure head offset due to contact sand. Vadose Zone J. 5, 1287–1292.

Reynolds, W.D., 2008. Unsaturated hydraulic properties: field tension infiltrometer. In: Carter, M.R., Gregorich, E.G. (Eds.), Soil Sampling and Methods of Analysis. Canadian Society of Soil Science & CRC Press Boca Raton, FL, pp. 1107–1128.

Reynolds, W.D., Topp, G.C., 2008. Soil water analyses: principles and parameters. In: Carter, M.R., Gregorich, E.G. (Eds.), Soil Sampling and Methods of Analysis. Canadian Society of Soil Science & CRC Press Boca Raton, FL, pp. 913–938.

Reynolds, W.D., Zebchuk, W.D., 1996. Use of contact material in tension infiltrometer measurements. Soil Technol. 9, 141–159.

Sauer, T.J., Clothier, B.E., Daniel, T.C., 1990. Surface measurements of the hydraulic properties of a tilled and untilled soil. Soil Tillage Res. 15, 359–369.

Schwarzel, K., Punzel, J., 2007. Hood infiltrometer — a new type of tension infiltrometer. Soil Sci. Soc. Am. J. 71, 1438–1447.

Skaggs, T.H., Wilson, G.V., Shouse, P.J., Leij, F.J., 2002. Solute transport: experimental methods. In: Dane, J.H., Topp, G.C. (Eds.), Methods of Soil Analysis: Physical Methods. Soil Science Society of America, Wisconsin, Madison, USA, pp. 1381–1402.

Smiles, D.E., Knight, J.H., 1976. A note on the use of the Philip infiltration equation. Aus. J. Soil Res. 14, 103–108.
Thony, J.L., Vachaud, G., Clothier, B.E., Angulo Jaramillo, R., 1991. Field measurement of the hydraulic properties of soil. Soil Technol. 4, 111–123.
Tillman, R.W., Scotter, D.R., Wallis, M.G., Clothier, B.E., 1989. Water repellency and its measurement by using intrinsic sorptivity. Aus. J. Soil Res. 27, 637–644.
Wallis, M.G., Scotter, D.R., Horne, D.J., 1991. An evaluation of the intrinsic sorptivity water repellency index on a range of New Zealand soils. Aus. J. Soil Res. 29, 353–362.
Wang, Z., Feyen, J., van Genuchten, M.T., Nielsen, D.R., 1998. Air entrapment effects on infiltration rate and flow instability. Water Resour. Res. 34, 213–222.